Magnus Willum Haakestad

Optical fibers with periodic structures

Thesis for the degree of philosophiae doctor

Trondheim, March 2006

Norwegian University of Science and Technology
Faculty of Information Technology, Mathematics and Electrical Engineering
Department of Electronics and Telecommunications

NTNU
Innovation and Creativity

NTNU
Norwegian University of Science and Technology

Thesis for the degree of philosophiae doctor

Faculty of Information Technology, Mathematics and Electrical Engineering
Department of Electronics and Telecommunications

ISBN 82-471-8130-4 (printed version)
ISBN 82-471-8129-0 (electronic version)
ISSN 1503-8181

Doctoral theses at NTNU, 2006:48

Printed by NTNU-trykk

Abstract

This thesis concerns some experimental and theoretical issues in fiber optics. In particular, properties and devices based on photonic crystal fibers (PCFs) are investigated.

The work can be grouped into three parts. In the first part we use sound to control light in PCFs. The lowest order flexural acoustic mode of various PCFs is excited using an acoustic horn. The acoustic wave acts as a traveling long-period grating. This is utilized to couple light from the lowest order to the first higher order optical modes of the PCFs. Factors affecting the acoustooptic coupling bandwidth are also investigated. In particular, the effect of axial variations in acoustooptic phase-mismatch coefficient are studied.

In the second part of the thesis we use an electric field to control transmission properties of PCFs. Tunable photonic bandgap guidance is obtained by filling the holes of an initially index-guiding PCF with a nematic liquid crystal and applying an electric field. The electric field introduces a polarization-dependent change of transmission properties above a certain threshold field. By turning the applied field on/off, an electrically tunable optical switch is demonstrated.

The third part consists of two theoretical works. In the first work, we use relativistic causality, i.e. that signals cannot propagate faster than the vacuum velocity of light, to show that Kramers-Kronig relations exist for waveguides, even when material absorption is negligible in the frequency range of interest. It turns out that evanescent modes enter into the Kramers-Kronig relations as an effective loss term. The Kramers-Kronig relations are particularly simple in weakly guiding waveguides as the evanescent modes of these waveguides can be approximated by the evanescent modes of free space. In the second work we investigate dispersion properties of planar Bragg waveguides with advanced cladding structures. It is pointed out that Bragg waveguides with chirped claddings do not give dispersion characteristics significantly different from Bragg waveguides with periodic claddings.

Acknowledgments

Most of the work in this thesis has been carried out at the Department of Electronics and Telecommunications at NTNU. I am grateful to the faculty and staff at the department for a stimulating working environment. In particular, I thank my main supervisor, Helge E. Engan, for his guidance and advice. His broad knowledge in optics and acoustics has also been of great help. I also wish to thank Johannes Skaar, for his collaboration on the theoretical work in this thesis. Some of the work would not have been possible without his mathematical insight. In addition, I would like to thank Bertil Nistad for his collaboration regarding the planar Bragg waveguides. I am also indebted to Astrid Aksnes, Kolbjørn Lindgjerdet, Therese McAdam, Andrea Raviglione, Steinar Smistad, Joar Sæther, and Bendik Vignes for their help.

A part of the work has been carried out at Research Center COM at DTU. I wish to thank the people at COM for their hospitality. I am in particular grateful to Anders Bjarklev for letting me into his group. I also thank my main collaborator at DTU, Thomas T. Alkeskjold, for his expertise with liquid crystal filled photonic crystal fibers, and Jesper Lægsgaard and Jesper Riishede for their helpful inputs regarding computer simulation of photonic crystal fibers. Finally, I thank Claus Friis Pedersen at NKT Research and Cato Fagermo at Crystal Fibre A/S for providing free fiber samples.

This work was financially supported by NFR and NorFA.

Contents

Chapter 1

Introduction

1.1 Background

Photonic crystal fibers, also called microstructured optical fibers, are optical fibers having a microstructure in the transverse plane. These fibers can guide light by means of total internal reflection, as in standard fibers, or by the photonic bandgap effect. There also exist fibers with a periodicity in the propagation direction of the light. Such fibers are called fiber gratings. The axial periodicity can induce coupling of light between co-propagating or counter-propagating modes.

Initial developments of PCFs

At about the same time as the standard, step index fiber was developed [1], it was realized that light could be guided in a silica core, surrounded by a microstructured air/silica cladding [2]. However, work on this type of fiber was abandoned due to the success of the step index fiber.

In the mid 1970s, a new type of guiding mechanism was proposed and analyzed by Yeh et al. [3–5]. They considered light guidance by Bragg scattering from a periodic cladding. This allows for light to be guided in a hollow core. The new type of fiber, called a Bragg fiber, did however prove difficult to fabricate, and little experimental progress was made during the following years.

The proposal that light can be confined in all three spatial dimensions due to the photonic bandgap effect [6, 7], stimulated much interest in photonic crystals [8]. The idea of using a photonic bandgap to trap light inspired Knight et al. to stack silica capillaries together in a hexagonal lattice, and draw them to a PCF with a solid core [9]. The first PCF did however not

guide light by the photonic bandgap effect. Instead, the air holes lowered the effective index of the periodic cladding, making the fiber guide light by total internal reflection [10]. An example of such an index-guiding PCF is shown in Fig. 1.1.

Figure 1.1: Cross-section of an index-guiding PCF.

By optimizing the PCF structure, true bandgap guidance was then demonstrated in a hollow core PCF [11]. However, the guided light was mainly located in silica in this fiber. This was overcome by Cregan et al. in 1999, who experimentally demonstrated bandgap guidance in air [12]. The first comprehensive theoretical analysis of air-guiding PCFs came shortly after [13].

It can be noted that there are several examples of photonic microstructures in nature. One example is the *Morpho rhetenor* butterflies, having highly reflective wings due to discrete multilayers of varying refractive index [14].

Applications of PCFs

Photonic crystal fibers have found a number of applications. A review of some properties and applications of PCFs can be found in Refs. [15–17].

Since bandgap guiding PCFs can guide light in an air core, the guided light is little affected by the absorption of 0.15 dB/km in silica. This suggests that air-guiding PCFs might find applications as transmission fibers. However, other loss mechanisms must be taken into consideration [18]. The lowest loss demonstrated to date is 13 dB/km in a single-mode air-guiding PCF [19], and 1.7 dB/km in a weakly multimode air-guiding PCF [20]. The

latter result is still about an order of magnitude larger than the loss of standard fibers.

Low loss alone is not sufficient for a successful transmission fiber; the effects of dispersion are also important for transmission at high bit rates. It has recently been shown theoretically that the waveguide dispersion of air core Bragg fibers can be tailored by introducing defects in the cladding [21].

Small-core index-guiding PCFs with high air fill fraction can have unusual dispersion properties in addition to high effective nonlinearity. Ranka et al. observed a broadening of the pulse spectrum when launching 100 fs pulses with 0.8 nJ energy into a 75 cm long PCF [22]. In fact, the wavelength spectrum of the pulse spanned over more than one octave after propagation through the fiber. This broadening, called supercontinuum generation, is caused by the combination of dispersion and nonlinearity of the PCF. Supercontinuum generation has found applications within frequency meteorology [23].

PCFs equivalent to double-clad fibers are useful within the field of high power fiber lasers and amplifiers [24, 25]. This is due to the possibility of having an outer cladding with high NA, allowing for high pump collection efficiency, and a large, active, single-mode signal core, reducing nonlinear effects.

Interesting physics and applications are found when filling the air holes with various materials. Low threshold stimulated Raman scattering has been demonstrated in a Hydrogen-filled air-core PCF [26]. Various devices, such as a variable optical attenuator, has been demonstrated by filling the air holes of a solid core PCF with polymers [27]. Another interesting possibility is to fill the air holes of an initially index-guiding PCF with a high-index liquid. This will turn the fiber into a bandgap guiding PCF. Tunable bandgap guidance has been demonstrated in such a fiber by varying the temperature [28]. Filling the air holes with liquid crystals is particularly interesting, since they can be highly sensitive to external perturbations [29].

Finally, it must be emphasized that advanced fully-vectorial simulation programs are of prime importance in the design of PCFs, due to the complexity of the PCF structures. An example of such a simulation model is given in Ref. [30].

Fiber gratings

While PCFs have a periodic structure in the transverse plane, fiber gratings are fibers having a periodically varying refractive index in the propagation direction of the light [31].

Consider a fiber where partly reflecting mirrors are placed periodically in the axial direction, with separation Λ. Maximum reflectivity occurs when the partial waves reflected from each mirror add up in phase. This gives the Bragg condition

$$\lambda_B = 2n_1\Lambda, \tag{1.1}$$

where λ_B is the Bragg wavelength, i.e. the wavelength of maximum reflectivity, and n_1 is the effective refractive index of the reflected mode.

The grating in the example above is called a short-period grating. There also exists a class of fiber gratings denoted long-period gratings, which couple light between co-propagating modes. In this case one may think of the grating consisting of periodically spaced scatterers, which scatter the light in the forward direction from e.g. mode 1 to mode 2. This gives the same condition as Eq. (1.1) for the wavelength of maximum coupling, except that $2n_1$ is replaced by $n_1 - n_2$, where n_1 and n_2 are the effective indices of mode 1 and 2, respectively. Since $2n_1 \gg n_1 - n_2$, it follows from Eq. (1.1) that the period of short-period gratings (typically about one micron) is much smaller than the period of long-period gratings (typically hundreds of microns).

One way of creating a long-period grating is to launch an acoustic wave along the fiber [32]. Thus, the fiber acts as a waveguide for both light and sound. The acoustic wave causes a periodic bending of the fiber, resulting in a long-period grating with the grating period equaling the acoustic wavelength. Hence, by adjusting the acoustic wavelength, one can tune the optical coupling wavelength. Long-period gratings have found several applications, e.g. as optical filters [33].

It is possible to make broadband and narrow-band filters by using fibers with optimized geometrical parameters [34]. Hence, tailoring fiber parameters using PCFs opens up the possibility of combining transverse and longitudinal periodicity for making new fiber devices [35, 36].

1.2 Outline

Chapter 2 and 3 give an introduction to fundamental characteristics of photonic crystal fibers and acoustooptic long-period fiber gratings, respectively. Chapter 4 summarizes the main results of the included papers and states the author's contributions. Conclusions are drawn in Chapter 5, together with suggestions for future work. The included papers constitute the main part of the Ph.D. work, and are collected in Appendix B.

Chapter 2

Photonic crystal fibers (PCFs)

Most PCFs fall into one of to classes, according to their guiding mechanism. The first type is index-guiding PCFs, which guide light by total internal reflection. The second type is bandgap guiding PCFs, which utilize the photonic bandgap effect to guide light. In this chapter, we will mainly focus on explaining the basics of the two types of guiding mechanisms.

2.1 Index-guiding PCFs

Consider the fiber in Fig. 1.1. This fiber is a pure silica cylinder with a number of air holes in it. The air holes are arranged in a triangular lattice with lattice spacing Λ. The diameter of the periodically spaced air holes is denoted d. The core consists of the absence of an air hole. Experimentally, it turns out that such a PCF guides only the fundamental mode when d/Λ is sufficiently small [10]. An example of the mode profile of the fundamental mode is shown in Fig. 2.1. The mode profile is calculated using a localized basis-function approach, where the field is written as a sum of Hermite-Gauss functions [37, 38].

2.1.1 Effective index model

There is a simple model, called the effective index model [10], which qualitatively explains the fundamental properties of index-guiding PCFs. The basic idea behind this model is to treat the index-guiding PCF as a standard step-index fiber, with an appropriately chosen effective cladding index, core

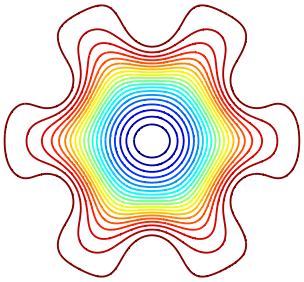

Figure 2.1: The fundamental mode of an index-guiding PCF.

index, and core radius. The important point for index-guiding PCFs is that the core index is higher than the effective cladding index, since the air holes lower the effective cladding index compared to the silica core. The effective cladding index is taken to equal the mode index of the fundamental mode of an infinite cladding. This mode is usually called the fundamental space-filling mode (FSM). The mode index of the FSM can effectively be found using numerical approaches, such as the plane-wave expansion method [30]. At short wavelengths, the field of the FSM is mainly located in silica, and n_{FSM} approaches the refractive index of silica. However, at long wavelengths, the field of the FSM extends into the air holes. n_{FSM} then approaches $fn_{\mathrm{air}} + (1-f)n_{\mathrm{si}}$, where f is the air-filling fraction of one unit cell in the cladding lattice [39]. Thus, the effective cladding index is strongly wavelength dependent.

The effective core index is n_{si}, since the core consists of the absence of an air hole. It is however not *a priori* obvious how to choose the effective core radius in the effective index model, except that it has to be of the order of magnitude one lattice spacing Λ. It turns out that an effective core radius $a_{\mathrm{eff}} \approx 0.6\Lambda$ gives best agreement between the effective index approach and results obtained by a fully vectorial solution of Maxwell's equations [40].

2.1.2 Effective V-parameter

Once n_{FSM} has been found numerically, one can compute the effective V-parameter for the PCF, defined as

$$V_{\mathrm{eff}} = \frac{2\pi}{\lambda} a_{\mathrm{eff}} \sqrt{n_{\mathrm{si}}^2 - n_{\mathrm{FSM}}^2}. \tag{2.1}$$

V_{eff} for hole diameters $d = 0.2\Lambda, 0.3\Lambda, \ldots, 0.8\Lambda$ is shown in Fig. 2.2 as a function of normalized frequency Λ/λ. The refractive index of silica is taken

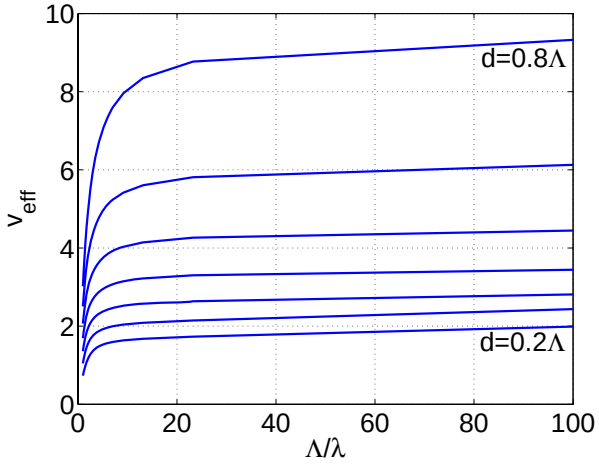

Figure 2.2: Effective V-parameter.

to be equal 1.444 in the calculation. An important thing to notice in the figure is that V_{eff} approaches a constant value at high frequencies. This is in strong contrast to standard step-index fibers, where V is proportional to λ^{-1}.

Standard step-index fibers are single-mode for $V < 2.4$. We observe from Fig. 2.2 that this criterion is satisfied for all frequencies when $d \leq 0.3\Lambda$. This prediction by the effective index model is in qualitative agreement with experiments and simulations [10, 41, 42]. It can be noted that the endlessly single-mode property can be utilized to make single-mode fibers with large mode area, simply by choosing a large value of Λ and a small value of d/Λ [43].

Furthermore, index-guiding PCFs can be designed to support the fundamental and second order modes over an practically infinite wavelength range [44]. To see this, consider a PCF with $d/\Lambda = 0.5$ and $\Lambda = 10$ μm. Such a PCF will have $V_{\text{eff}} \approx 2.9 \ldots 3.5$ for $\lambda < 2$ μm, according to Fig. 2.2. This is above the second-order mode cutoff at $V = 2.4$, but below the third-order mode cutoff at $V = 3.8$. This practically endlessly two-mode property is an attractive feature for two-mode devices. In must however be kept in mind that other issues, such as macrobending loss [45], also have to be taken into consideration.

It is also possible to make index-guiding PCFs with very small mode area [46]. This can be done by choosing a high air-fill fraction, e.g. $d = 0.8\Lambda$, to obtain a large index contrast between the core and the cladding, and a

small hole spacing $\Lambda \approx \lambda$, to obtain a small effective core diameter. Such a fiber can be thought of as a silica rod of diameter $\sim \Lambda$, suspended in air. The large effective index contrast and small core diameter will lead to a tightly confined mode. This confinement results in high intensity for a given optical power, leading to enhanced nonlinear effects. An example of this type of PCF is shown in Fig. 2.3(a).

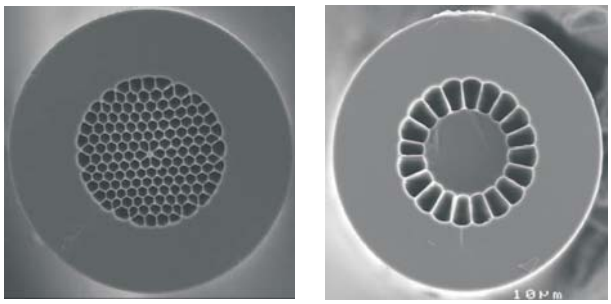

Figure 2.3: A small-core PCF (a) and a multimode PCF (b). Pictures appear courtesy of Crystal Fibre A/S.

Finally, consider an index-guiding PCF with high air-fill fraction and large hole spacing. Such a fiber will be multimode, according to Fig. 2.2. This kind of PCF is useful for guiding high powers due to a low intensity for a given optical power. Figure 2.3(b) shows a variation of such a PCF.

2.2 Bandgap guiding PCFs

The second main type of PCFs guide light by the photonic bandgap effect. We will first give an introduction to photonic bandgaps, and then discuss the basic properties of bandgap guiding waveguides. For simplicity, focus is placed on planar Bragg waveguides. Based on the properties of planar Bragg waveguides, we will briefly consider bandgap guiding PCFs.

2.2.1 Bloch's theorem and photonic bandgaps

Here some general properties of light in periodic media is presented. Much of the formalism is similar to that of electrons in solid state physics [47].

Consider electromagnetic fields in an isotropic, non-magnetic, non-dispersive, lossless, linear medium, with no free charges and currents. A time dependence $\exp(-i\omega t)$ is assumed for the electric and magnetic fields. In this case,

the equation for the magnetic field $\mathbf{H}$ becomes

$$\nabla \times \left[\frac{1}{\epsilon_r(\mathbf{r})} \nabla \times \mathbf{H}(\mathbf{r}) \right] = \left(\frac{\omega}{c} \right)^2 \mathbf{H}(\mathbf{r}), \tag{2.2}$$

where ϵ_r is the relative permittivity. We notice that this equation takes the form of an eigenvalue problem, where $\mathbf{H}$ is the eigenvector and ω^2/c^2 is the eigenvalue. In fact, it can be shown that the operator on the left hand side of Eq. (2.2) is Hermitian [8]. Consequently, all properties of Hermitian operators, which are well-known in quantum mechanics, applies here. One important property is that the eigenvalues are real, and that the eigenvectors are orthogonal. The reader is referred to general quantum mechanics textbooks, such as Ref. [48], for a discussion of some further properties, such as simultaneous diagonalization of commuting operators, the variational theorem, and first order perturbation theory.

We then assume that the permittivity is periodic, i.e. that

$$\epsilon_r(\mathbf{r} + \mathbf{R}) = \epsilon_r(\mathbf{r}), \tag{2.3}$$

where $\mathbf{R}$ is a lattice vector. According to Bloch's theorem [8], one then has

$$\mathbf{H}(\mathbf{r}) = \mathbf{u}_\mathbf{k}(\mathbf{r}) e^{i\mathbf{k}\cdot\mathbf{r}}, \tag{2.4}$$

where

$$\mathbf{u}_\mathbf{k}(\mathbf{r} + \mathbf{R}) = \mathbf{u}_\mathbf{k}(\mathbf{r}). \tag{2.5}$$

Thus, the eigenvectors take the form of a plane wave modulated by a periodic function $\mathbf{u}_\mathbf{k}$, which has the same periodicity as ϵ_r. The Bloch vector $\mathbf{k}$ defines the direction of the Bloch wave. Note that $\mathbf{k}$ has to be real in an infinite photonic crystal; if it is complex, the Bloch wave will increase exponentially for some direction, which is unphysical in an infinite crystal. A range of frequencies where there are no real values of $\mathbf{k}$ is denoted a photonic bandgap.

Consider then a semi-infinite photonic crystal, which occupies the region $x > 0$. We assume that a plane wave with wave vector $[k_x, 0, 0]$, is incident on this structure. It is assumed that the frequency of the plane wave is within the bandgap of the photonic crystal. Now since the photonic crystal is semi-infinite, a complex Bloch vector $[k + i\kappa, 0, 0]$, where $\kappa > 0$, is allowed, since this will lead to an exponentially decaying Bloch wave $\mathbf{u}_\mathbf{k} \exp(ikx) \exp(-\kappa x)$ in the $+x$-direction, but no unlimited exponential increase in the opposite direction, since the photonic crystal only occupies the $x > 0$ region. Due to energy conservation, it then follows that all light must be reflected by the

photonic crystal. This leads to the conclusion that a semi-infinite photonic crystal acts as a perfectly reflecting mirror for a plane wave impinging on it from the outside, for frequencies within the bandgap. This effect is utilized in bandgap-guiding fibers, where the photonic crystal cladding acts as a highly reflecting mirror for a certain range of frequencies and propagation constants.

2.2.2 Planar Bragg waveguides

The simplest example of a bandgap guiding waveguide is the planar Bragg reflection waveguide [3], where a hollow core is surrounded by a periodic cladding consisting of an infinite number of alternating high and low index layers. As a specific example, consider the symmetric Bragg reflection waveguide in Fig. 2.4. Since the waveguide is symmetric, the modes are either symmetric or anti-symmetric [8], and we therefore only need to consider one half of the waveguide structure, say $y > 0$. The index of refraction is 1.5 in the high index layers and 1 in the low index layers. Consider a TE-polarized plane wave with frequency ω and wave vector $[0, k_y, \beta]$ incident on the periodic cladding. Due to continuity of the E-field, a Bloch wave with Bloch vector $[0, k + i\kappa, \beta]$ and frequency ω is excited in the cladding. $k + i\kappa$ is determined by β and ω. It is useful to map out values of (β, ω) where $\kappa > 0$. In these regions, the Bloch wave is evanescent in the y-direction, and an incoming plane wave will be reflected from the cladding. The bandgaps are shown in yellow in Fig. 2.5.

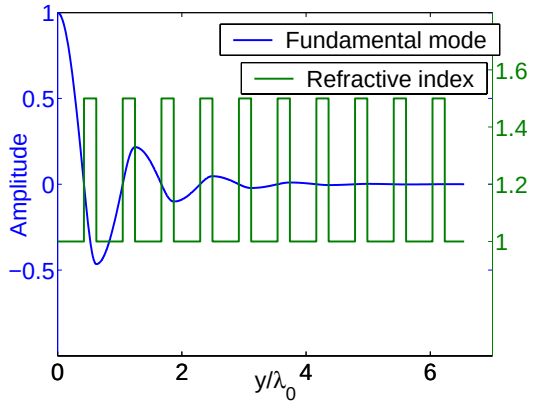

Figure 2.4: The fundamental TE-mode at $\lambda = \lambda_0$, and the refractive index profile of a symmetric Bragg reflection waveguide. λ_0 is an arbitrary length.

A guided mode in the Bragg reflection waveguide can be thought of as a plane wave bouncing back and forth in the core, forming a standing wave pattern. Two conditions must be satisfied for this to happen. The first condition is that all light is reflected from the cladding, i.e. that the (β, ω) value of the mode is within a bandgap. The second requirement is that the plane wave should interfere constructively with itself after one round trip. This phase match condition yields the dispersion relation, $\omega(\beta)$, of the mode. From the dispersion relation, one can determine the mode index, group velocity, and dispersion coefficient. The dispersion relations for lowest order modes of the Bragg reflection waveguide are shown in dark blue in Fig. 2.5. The mode profile of the fundamental mode at the wavelength λ_0

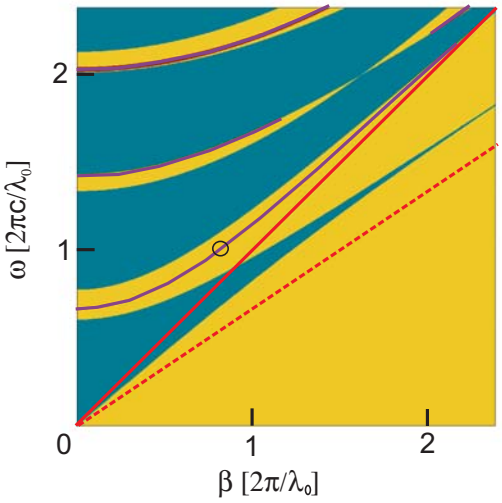

Figure 2.5: Band diagram for TE-polarized light in the planar Bragg reflection waveguide.

is shown in Fig. 2.4. The corresponding point in the dispersion diagram is shown as a black circle in Fig. 2.5.

Note that one must have $\omega > c\beta$ in order to have a core-guided mode, otherwise the field would be evanescent in the core. The line $\omega = c\beta$ is the solid red line in Fig. 2.5. The dotted red line shows $\omega = (c/1.5)\beta$. In the region $c\beta > \omega > (c/1.5)\beta$, the fields are evanescent in the low index layers, but harmonically varying in the high index layers. In this case, each high index layer acts as an index-guiding waveguide. The cladding can then be thought of as an infinite number of coupled index-guiding waveguides [4].

Below the line $\omega = (c/1.5)\beta$, the fields are evanescent in both the high and low index layers, and no solutions of Eq. (2.2) exist.

2.2.3 Air-guiding PCFs

An example of an air-guiding PCF is shown in Fig. 2.6. This type of fiber

Figure 2.6: An air-guiding PCF. Picture appear courtesy of Crystal Fibre A/S.

guides light by the same mechanism as the Bragg reflection waveguide, that is, the cladding acts as a mirror for (β, ω) values in the photonic bandgap. A typical band diagram of such a fiber is given in Ref. [13]. However, the finite number of cladding layers cause leakage of light out of the core. This loss mechanism can be reduced to less than 0.1 dB/km by choosing a sufficiently large number of cladding layers [49]. Furthermore, material absorption in silica causes less loss than for standard fibers, since most of the light propagates in air. It has recently been suggested that surface roughness determines the ultimate limit to the loss [18], and that the attenuation of 1.7dB/km, in the lowest loss air-guiding PCFs reported [20], is already dominated by this loss mechanism.

Chapter 3

Acoustooptic fiber gratings

Coupled mode theory is an useful alternative to the Bloch-wave formalism when treating fibers with a periodically varying refractive index in the propagation direction of the light [50]. This chapter considers the application of coupled mode theory to optical fiber devices that use a traveling flexural acoustic wave to couple light between two co-propagating optical modes.

3.1 Perturbation due to an acoustic wave

An optical fiber with the coating removed can as a first approximation be regarded acoustically as a homogeneous cylinder. There are generally three types of acoustic modes in homogeneous cylinders: Torsional, flexural, and longitudinal [51]. Here we will consider the lowest order flexural mode in the low frequency regime, i.e. when

$$fa/c_t \ll 1, \tag{3.1}$$

where f is the acoustic frequency, a is the fiber radius, and c_t is the transverse acoustic wave velocity in silica, which is 3764 m/s. The condition in Eq. (3.1) corresponds to $f \ll 60$ MHz for a fiber radius of 62.5 μm.

The lowest order flexural acoustic mode causes a periodic bending of the fiber in the low frequency regime [52], and the displacement can be approximated by [53]

$$u(x, y, z, t) = u_0 \cos(Kz - \Omega t)\hat{\mathbf{x}}. \tag{3.2}$$

Here the acoustic wave is taken to be polarized in the x-direction. From energy conservation, the relation between the amplitude u_0 and the power

carried by the acoustic wave is [51]

$$P = 4\rho(\pi^7 c_{\text{ext}} a^5 f^5)^{1/2} u_0^2, \tag{3.3}$$

where the density ρ of silica is 2200 kg/m^3, and $c_{\text{ext}} = 5760$ m/s. We note that the power is proportional to the square of the acoustic amplitude. Typically, the amplitude of the acoustic wave is of the order of magnitude 1 nm. This gives a power of 36 mW, assuming an acoustic frequency of 10 MHz and a fiber radius of 62.5 μm.

The dispersion relation for the lowest order flexural mode in the low frequency regime is [52]

$$\Lambda_a = (\pi a c_{\text{ext}}/f)^{1/2}, \tag{3.4}$$

where Λ_a is the acoustic wavelength. For example, $f = 10$ MHz and $a = 62.5$ μm give $\Lambda_a = 0.3$ mm.

The acoustic wave perturbs the fiber in two ways. The first effect is an asymmetrical change is optical path length due to the bending of the fiber. The second effect is a change in the refractive index of silica due to the elasto-optic effect. The combination of these two effects causes a perturbation [53, 54]

$$\Delta n(x, y, z, t) = \Delta n(x, y) \cos(Kz - \Omega t), \tag{3.5}$$

where

$$\Delta n(x, y) = n_0(1 + \chi) K^2 u_0 x. \tag{3.6}$$

Here $\chi = -0.22$ is for silica, which expresses the reduction in Δn due to the elasto-optic effect, and n_0 is the refractive index profile of the unperturbed fiber.

The acoustic wave is quickly damped in the fiber coating. This implies that the acoustooptic interaction region is defined by the stripped part of the fiber, as shown in Fig. 3.1.

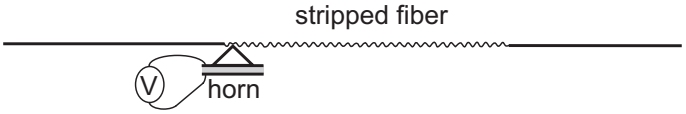

Figure 3.1: An acoustic wave traveling in the stripped part of a fiber.

3.2 Coupled mode equations

It is assumed that the acoustic wave couples light between two optical modes, denoted mode 1 and mode 2. Coupling to all other modes is neglected. The electric field in the stripped fiber section can then be represented as a superposition of mode 1 and mode 2

$$\psi(\mathbf{r},t) = \sum_{i=1}^{2} a_i(z)\psi_i(x,y)\exp\left[i(\beta_i z - \omega_i t)\right]. \tag{3.7}$$

A scalar notation is used here for simplicity. a_i, ψ_i, β_i, and ω_i denote mode weight, normalized mode profile, propagation constant, and angular frequency, respectively, for mode i. It can be shown that the angular frequencies of the coupled modes must satisfy [50]

$$\omega_1 = \omega_2 + \Omega. \tag{3.8}$$

This frequency shift can be thought of as a Doppler shift due to the traveling acoustic wave.

It can also be shown that the electric field evolves according to the coupled mode equations [50]

$$\frac{\mathrm{d}a_1(z)}{\mathrm{d}z} = i\kappa a_2(z)\exp(-i\Delta\beta z) \tag{3.9}$$

$$\frac{\mathrm{d}a_2(z)}{\mathrm{d}z} = i\kappa a_1(z)\exp(i\Delta\beta z), \tag{3.10}$$

where the acoustooptic phase-mismatch coefficient $\Delta\beta$ is given by

$$\Delta\beta = \beta_1 - \beta_2 - K, \tag{3.11}$$

and κ is the acoustooptic coupling constant, which is given by

$$\kappa \approx \frac{k_1}{2}\langle\psi_2|\Delta n(x,y)|\psi_1\rangle, \tag{3.12}$$

where $k_1 = \omega_1/c$. An important thing to notice is that since the perturbation $\Delta n(x,y)$ is anti-symmetric with respect to the x-axis, one only obtains a non-zero coupling coefficient between symmetric and anti-symmetric modes (with respect to the x-axis). For example, one may couple light between the symmetric LP_{01} mode and the anti-symmetric LP_{11} mode.

From Eqs. (3.9)-(3.10), we find that

$$\frac{d}{dz}\left(|a_1(z)|^2 + |a_2(z)|^2\right) = 0, \tag{3.13}$$

that is, an increase of the power in mode 1 is always accompanied by a decrease of the power in mode 2, and vice versa.

We will consider three cases. In all cases it is assumed that $a_1(0) = 1$ and $a_2(0) = 0$.

a_1 constant

The case $a_1(z) \approx 1$ is considered first. This is relevant when the coupling is too weak to cause significant transfer of energy from mode 1 to mode 2 over the acoustooptic interaction region. We can then integrate Eq. (3.10) directly and obtain

$$|a_2(L)|^2 = (\kappa L)^2 \mathrm{sinc}^2\left(\frac{\Delta\beta L}{2}\right), \tag{3.14}$$

Where L is the length of the acoustooptic interaction region. The bandwidth is found by considering the first zero of the sinc function. This gives

$$|\Delta\beta| < \frac{2\pi}{L}, \tag{3.15}$$

which shows that the bandwidth is inversely proportional to the length of the acoustooptic interaction region.

$\Delta\beta = 0$

The condition $\Delta\beta = 0$ is denoted perfect phase-match. Inserting $\Delta\beta = 0$ into Eqs. (3.9) and (3.10) gives, using the initial conditions, that

$$|a_1(L)|^2 = \cos^2(\kappa L) \tag{3.16}$$
$$|a_2(L)|^2 = \sin^2(\kappa L), \tag{3.17}$$

which shows that light is coupled periodically from mode 1 to mode 2, and vice versa. All light is coupled from one mode to the other after a length

$$L = \frac{\pi}{2\kappa}. \tag{3.18}$$

Note that $\Delta\beta = 0$ corresponds to the Bragg condition Eq. (1.1). The proof of this is left to the reader.

General case

By solving the coupled mode equations exactly using the the initial conditions, we obtain

$$|a_2(L)|^2 = \frac{\kappa^2}{\kappa^2 + \left(\frac{\Delta\beta}{2}\right)^2} \sin^2\left(\sqrt{\kappa^2 + \left(\frac{\Delta\beta}{2}\right)^2}\, L\right). \tag{3.19}$$

A plot of $|a_2(L)|^2$ when $\kappa L = \pi/2$ is shown in Fig. 3.2.

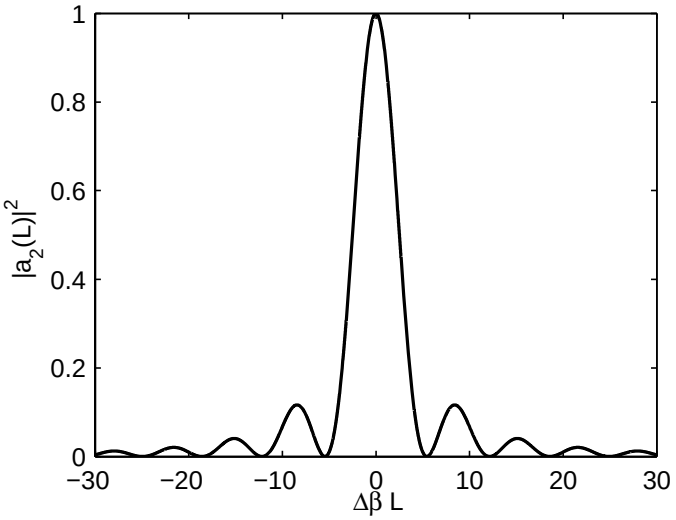

Figure 3.2: Fraction of light coupled to mode 2 when $\kappa L = \pi/2$.

3.2.1 Coupling bandwidth

We will finally take a closer look at the acoustooptic coupling bandwidth [55]. It is assumed that $\kappa L = \pi/2$, i.e. that all light is coupled from mode 1 to mode 2 at the end of the interaction region when $\Delta\beta = 0$. We wish to find the range of $|\Delta\beta|$ satisfying

$$|a_2(L)|^2 > \frac{1}{2}. \tag{3.20}$$

This gives from Eq. (3.19) that

$$|\Delta\beta| < \frac{2.5}{L}. \tag{3.21}$$

This is somewhat less than Eq. (3.15) due to a different definition of the bandwidth.

We then use that

$$\Delta\beta(\lambda, f) = 2\pi \left(\frac{1}{L_b(\lambda)} - \frac{1}{\Lambda_a(f)} \right), \tag{3.22}$$

where L_b is the intermodal beatlength between mode 1 and 2. Note that $\Delta\beta$ is a function of both λ and f. The most common situation takes place when the acoustic frequency is constant, and the transmission $1-|a_2(L)|^2$ is recorded as a function of optical wavelength using e.g. broadband light and an optical spectrum analyzer. In this case we write $\Delta\beta = \Delta\beta(\lambda)$. Assuming that $\Delta\beta(\lambda_0) = 0$, we can Taylor expand $L_b(\lambda)$ to first order around λ_0 obtaining

$$\Delta\beta(\lambda) \approx -\frac{2\pi L_b'(\lambda_0)\Delta\lambda}{L_b^2(\lambda_0)}, \tag{3.23}$$

where $\Delta\lambda = \lambda - \lambda_0$. Inserting this into Eq. (3.21), we obtain

$$\Delta\lambda_{\mathrm{FWHM}} = \frac{0.8}{L} \frac{L_b^2(\lambda_0)}{|L_b'(\lambda_0)|}, \tag{3.24}$$

where $\Delta\lambda_{\mathrm{FWHM}}$ is the FWHM coupling bandwidth.

We note from Eq. (3.24) that there are two factors determining the coupling bandwidth. The first factor is the length L of the acoustooptic interaction region. L must be in the range from 1 cm to 100 cm in practice: Power requirements and damping of the acoustic wave outside the acoustooptic interaction region limit the minimum length, while acoustic damping along the stripped fiber and practical device sizes limit the maximum length. However, the coupling bandwidth is also determined by the fiber properties through the term $L_b^2(\lambda_0)/|L_b'(\lambda_0)|$. This term can be tailored by optimizing the fiber geometry. This makes PCFs useful for making acoustooptic devices, since they provide freedom in tailoring fiber properties.

Chapter 4

Summary of papers

This chapter gives an overview of each included paper. We also provide the motivation for the papers and state the author's contributions. The included papers are denoted Paper A, Paper B, and so on.

4.1 Acoustooptic experiments

The main motivation behind these experiments was to investigate to what extent characteristics of index-guiding photonic crystal fibers affect the properties of acoustooptic long-period fiber gratings. One such property is the acoustooptic coupling bandwidth [34]. Tailoring the coupling bandwidth might be useful in acoustooptic tunable filters for use as dynamic gain-flattening devices for Erbium-doped fiber amplifiers [56].

Paper A: Acoustooptic properties of a weakly multimode solid core photonic crystal fiber

This paper reports a measurement of the phase velocity for the lowest order flexural acoustic mode for both a solid core and a hollow core PCF, and a measurement of the intermodal beat length between the lowest order and first four nearly degenerate higher order optical modes of the solid core PCF. The measurements of acoustic phase velocity and optical beat length were seen to be in good agreement with calculations. There was a broadening of the notches in the optical transmission spectra at increased acoustic frequency. This is likely caused by the combined effect of fiber imperfections and splitting in mode index between the four nearly degenerate higher order modes for a perfect structure.

I performed the simulations and experiments, and wrote the paper.

Paper B: Acoustooptic characterization of a birefringent two-mode photonic crystal fiber

It is critical that fibers used in acoustooptic tunable filters are axially uniform, since axial non-uniformities may give rise to significant sidelobes in the transmission spectrum [57–59]. We therefore investigated to what extent axial variations in acoustooptic phase-mismatch coefficient contributed to the acoustooptic coupling bandwidth in a birefringent two-mode PCF. A method is presented, where axial variations in the acoustooptic phase-mismatch coefficient are obtained directly from the transmission spectrum. This method is compared to an existing method where axial non-uniformities are measured using acoustic pulses [59]. The two methods are found to be in good agreement. The measurements show that the minimum coupling bandwidth was limited by axial variations in acoustooptic phase-mismatch coefficient.

I performed the simulations and experiments, and wrote the paper.

4.2 Electrical tuning of photonic bandgaps

This work was carried out in collaboration with Thomas T. Alkeskjold during a stay at DTU in the spring of 2004. The original plan was to use a flexural acoustic wave to control transmission properties of a liquid crystal filled PCF. Previously, Larsen et al. had shown that temperature tuning and highly sensitive thermal switching of a photonic bandgap fiber could be accomplished with a liquid crystal filled PCF [29]. The initial acoustic experiments were unsuccessful, and the focus was turned to electrical tuning instead. Such a device could possibly find applications within polarization control.

Paper C: Electrically tunable photonic bandgap guidance in a liquid-crystal-filled photonic crystal fiber

In this paper we demonstrate that tunable bandgap guidance can be obtained by filling the holes of an initially index-guiding solid core PCF with a nematic liquid crystal, and applying an electric field. A polarization dependent change in optical transmission properties was observed above a threshold field, and the response times were found to be in the ms range. The insertion loss was 1.3 dB at 1500 nm wavelength, in addition to the splice loss.

I performed the experiments and wrote the paper.

4.3 Origin and properties of waveguide dispersion

The effects of dispersion are crucial for a range of applications such as transmission at high bit rates, dispersion compensation, and enhancement or suppression of nonlinear effects. In order to exploit the potential of microstructured fibers, it is therefore important to understand the origin of waveguide dispersion. The first of our studies was also motivated by the fact that photonic bandgap fibers can have large values of waveguide dispersion, in addition to sharp transmission features [60]. Consequently, it was of interest to find out if Kramers-Kronig relations similar to those for homogeneous media exist for waveguides. The main motivation for the second study was to investigate dispersion properties of planar Bragg waveguides with advanced cladding profiles. Since many of the characteristics of Bragg fibers are similar to those of the planar case, the results could also be useful for Bragg fibers.

Paper D: Causality and Kramers–Kronig relations for waveguides

It is shown that Kramers-Kronig relations exist for waveguides, even when material dispersion and material loss is negligible in the frequency range of interest. The theory is applied to hollow waveguides with perfectly conductive walls, index-guiding dielectric waveguides, and bandgap-guiding waveguides. We demonstrate that for hollow waveguides with perfectly conductive walls, each mode propagates causally, and the associated mode index obeys the usual Kramers-Kronig relations. That is, the real part of the mode index is determined by the imaginary part, and vice versa. For dielectric waveguides, it turns out that the (real) mode index of a guided mode is related to the (imaginary) mode indices of the evanescent modes. For weakly guiding waveguides, we show that the derivative of the mode index with respect to frequency for a certain mode is given solely by the associated mode field profile.

The theory was developed in collaboration with Johannes Skaar. I performed the simulations, and wrote the paper.

Paper E: Dispersion properties of planar Bragg waveguides

In this paper we study some properties of planar Bragg waveguides with a finite number of cladding layers. We show that the leaky mode condition (no incoming flux from the outermost layer) can be reformulated as a phase match condition, similarly to that of conventional, planar dielectric waveguides. We also give a simple, approximate formula for the loss.

These relations are useful as they enable efficient analysis of the modes. A general expression for the waveguide dispersion can be derived using the phase match condition. With the help of this expression and numerical calculations, we explain that chirped claddings do not give dispersion characteristics significantly different from waveguides with periodic claddings. This is an important result as it shows that dispersion tailoring cannot be achieved in a similar way as with fiber Bragg gratings or thin-film filters. Also, in order to understand the dispersion characteristics of other waveguides with non-periodic claddings, we consider waveguides with high-index defects close to the core [61].

I wrote an initial version of the simulation program, contributed at least half to the theory, and contributed to the writing of the paper.

Chapter 5

Conclusions and outlook

In summary, several properties and devices based on photonic crystal fibers have been studied in this thesis. Based on the results obtained, we will here draw some conclusions, make suggestions for further work, and comment on some recent developments.

Regarding the acoustooptic experiments, it was found that the acoustooptic coupling bandwidth was larger than expected for coupling to a single mode in a perfect fiber. This is an undesired feature for narrow-band acoustooptic tunable filters. For the birefringent PCF, the broadening in acoustooptic coupling bandwidth was due to axial variations in the acoustooptic phase-mismatch coefficient. A natural next step would be to investigate the cause of these variations. One could, for example, use a laser probe to measure axial variations in fiber thickness, in order to check if this is the cause of the axial variations in acoustooptic phase-mismatch coefficient. If so, acoustooptic coupling could find applications as a tool for performing quality checks of fabricated PCFs.

It would also be interesting to study acoustooptic coupling in photonic bandgap fibers, since these fibers have properties radically different from index-guiding PCFs. Long-period gratings in bandgap-guiding PCFs have recently been demonstrated using periodic microbending [62].

Finally, a promising new idea is to study Brillouin scattering in small-core PCFs with high air fill-fraction. In such fibers, the core can approximately be regarded acoustically as a glass cylinder suspended in air. This will modify the dispersion relation of the acoustic phonons and thereby alter the properties of Brillouin scattering [63].

PCFs filled with liquid crystals are candidates for highly tunable and compact fiber devices [64]. In the work using an applied voltage to control

transmission properties of liquid crystal filled PCFs, it was found that the optical transmission properties could be altered above a certain threshold field. However, a complete computer simulation of the resulting polarization-dependent transmission was not performed. One important step would therefore be to reproduce the observed transmission properties theoretically. Some computer simulations of liquid crystal filled PCFs have already been performed [65, 66].

There could be several potential applications of voltage-controlled liquid crystal filled PCFs, e.g. within polarization control, as tunable polarizers, and as electric field sensors.

Some recent work has utilized different anchoring conditions to avoid a threshold field, and to avoid reverse tilt domains [67]. Optically induced thermal tuning has also recently been demonstrated [68].

Using the principle of relativistic causality, we found that Kramers-Kronig relations exist for waveguides, even with negligible material absorption in the frequency range of interest. The crucial point is that evanescent modes act as an effective loss term in these relations.

There are several ways in which this work could be extended. An important question is that of completeness for absorbing waveguides. It would be useful to identify the exact conditions under which completeness holds for the normal modes of a general absorbing waveguide. Some work regarding completeness in absorbing waveguides has previously been performed [69, 70]. In addition, studying Kramers-Kronig relations in weakly guiding waveguides with weak absorption could find useful applications. In this case, the Kramers-Kronig relations could be used as a new method to determine dispersion by measuring the mode field of a given mode as a function of wavelength using e.g. a tunable laser and a CCD camera. This would make it possible to measure dispersion using very short (on the order of 10 cm) fiber sections.

Regarding dispersion properties of planar waveguides, it would be natural to consider how the results would apply to Bragg fibers and bandgap-guiding PCFs. For air-core bandgap fibers, it has been found that the loss is dominated by surface roughness, and that this effect can be reduced by increasing the diameter of the core [18]. This will unfortunately make the fibers multimode. However, a new and interesting idea is to introduce defects close to the core to obtain large loss for all higher order modes, except for the fundamental mode [71]. This seems like a possible route for making low-loss air-core bandgap fibers.

Bibliography

[1] D. B. Keck, R. D. Maurer, and P. C. Schultz, "Ultimate lower limit of attenuation in glass optical waveguides," *Appl. Phys. Lett.*, vol. 22, pp. 307–309, 1973.

[2] P. Kaiser, E. A. J. Marcatili, and S. E. Miller, "A new optical fiber," *Bell Syst. Tech. J.*, vol. 52, pp. 265–269, Feb. 1973.

[3] P. Yeh and A. Yariv, "Bragg reflection waveguides," *Opt. Commun.*, vol. 19, pp. 427–430, Dec. 1976.

[4] P. Yeh, A. Yariv, and C.-S. Hong, "Electromagnetic propagation in periodic stratified media. I. General theory," *J. Opt. Soc. Am.*, vol. 67, pp. 423–438, Apr. 1977.

[5] P. Yeh, A. Yariv, and E. Marom, "Theory of Bragg fiber," *J. Opt. Soc. Am.*, vol. 68, pp. 1196–1201, Sept. 1978.

[6] E. Yablonovitch, "Inhibited spontanous emission in solid-state physics and electronics," *Phys. Rev. Lett.*, vol. 58, pp. 2059–2062, May 1987.

[7] S. John, "Strong localization of photons in certain disordered dielectric superlattices," *Phys. Rev. Lett.*, vol. 58, pp. 2486–2489, June 1987.

[8] J. D. Joannopoulos, J. N. Winn, and R. D. Meade, *Photonic Crystals: Molding the Flow of Light*. Princeton: Princeton Univ. Press, 1995.

[9] J. C. Knight, T. A. Birks, P. S. J. Russell, and D. M. Atkin, "All-silica single-mode optical fiber with photonic crystal cladding," *Opt. Lett.*, vol. 21, pp. 1547–1549, Oct. 1996.

[10] T. A. Birks, J. C. Knight, and P. S. J. Russell, "Endlessly single-mode photonic crystal fiber," *Opt. Lett.*, vol. 22, pp. 961–963, July 1997.

[11] J. C. Knight, J. Broeng, T. A. Birks, and P. S. J. Russell, "Photonic band gap guidance in optical fibers," *Science*, vol. 282, pp. 1476–1478, Nov. 1998.

[12] R. F. Cregan, B. J. Mangan, J. C. Knight, T. A. Birks, P. S. J. Russell, P. J. Roberts, and D. C. Allan, "Single-mode photonic band gap guidance of light in air," *Science*, vol. 285, pp. 1537–1539, Sept. 1999.

[13] J. Broeng, S. E. Barkou, T. Søndergaard, and A. Bjarklev, "Analysis of air-guiding photonic bandgap fibers," *Opt. Lett.*, vol. 25, pp. 96–98, Jan. 2000.

[14] P. Vukusic and J. R. Sambles, "Photonic structures in biology," *Nature (London)*, vol. 424, pp. 852–855, Aug. 2003.

[15] J. Broeng, D. Mogilevstev, S. E. Barkou, and A. Bjarklev, "Photonic crystal fibers: A new class of optical waveguides," *Optical Fiber Technology*, vol. 5, pp. 305–330, 1999.

[16] P. Russell, "Photonic crystal fibers," *Science*, vol. 299, pp. 358–362, Jan. 2003.

[17] J. Lægsgaard and A. Bjarklev, "Microstructured optical fibers–Fundamentals and applications," *J. Am. Ceram. Soc.*, vol. 89, pp. 2–12, Jan. 2006.

[18] P. J. Roberts, F. Couny, H. Sabert, B. J. Mangan, D. P. Williams, L. Farr, M. W. Mason, A. Tomlinson, T. A. Birks, J. C. Knight, and P. S. J. Russell, "Ultimate low loss of hollow-core photonic crystal fibres," *Opt. Express*, vol. 13, pp. 236–244, Jan. 2005.

[19] C. M. Smith, N. Venkataraman, M. T. Gallagher, D. Müller, J. A. West, N. F. Borrelli, D. C. Allan, and K. W. Koch, "Low-loss hollow-core silica/air photonic bandgap fibre," *Nature (London)*, vol. 424, pp. 657–659, Aug. 2003.

[20] B. J. Mangan, L. Farr, A. Langford, P. J. Roberts, D. P. Williams, F. Couny, M. Lawman, M. Mason, S. Coupland, R. Flea, H. Sabert, T. A. Birks, J. C. Knight, and P. S. J. Russell, "Low loss (1.7 dB/km) hollow core photonic bandgap fiber," in *Proc. Opt. Fiber Commun. Conf.*, Los Angeles, CA, 2004, paper PDP24.

[21] T. D. Engeness, M. Ibanescu, S. G. Johnson, O. Weisberg, M. Skorobogatiy, S. Jacobs, and Y. Fink, "Dispersion tailoring and compensation by modal interactions in omniguide fibers," *Opt. Express*, vol. 11, pp. 1175–1196, May 2003.

[22] J. K. Ranka, R. S. Windeler, and A. J. Stentz, "Visible continuum generation in air-silica microstructure optical fibers with anomalous dispersion at 800 nm," *Opt. Lett.*, vol. 25, pp. 25–27, Jan. 2000.

[23] T. Udem, R. Holzwarth, and T. W. Hänsch, "Optical frequency metrology," *Nature (London)*, vol. 416, pp. 233–237, Mar. 2002.

[24] K. Furusawa, A. Malinowski, J. H. V. Price, T. M. Monro, J. K. Sahu, J. Nilsson, and D. J. Richardson, "Cladding pumped Ytterbium-doped fiber laser with holey inner and outer cladding," *Opt. Express*, vol. 9, pp. 714–720, Dec. 2001.

[25] J. Limpert, A. Liem, M. Reich, T. Schreiber, S. Nolte, H. Zellmer, A. Tünnermann, J. Broeng, A. Petersson, and C. Jakobsen, "Low-nonlinearity single-transverse-mode ytterbium-doped photonic crystal fiber amplifier," *Opt. Express*, vol. 12, pp. 1313–1319, Apr. 2004.

[26] F. Benabid, J. C. Knight, G. Antonopoulos, and P. S. J. Russell, "Stimulated Raman scattering in hydrogen-filled hollow-core photonic crystal fiber," *Science*, vol. 298, pp. 399–402, Oct. 2002.

[27] B. J. Eggleton, C. Kerbage, P. S. Westbrook, R. S. Windeler, and A. Hale, "Microstructured optical fiber devices," *Opt. Express*, vol. 9, pp. 698–713, Dec. 2001.

[28] R. T. Bise, R. S. Windeler, K. S. Kranz, C. Kerbage, B. J. Eggleton, and D. J. Trevor, "Tunable photonic band gap fiber," in *Optical Fiber Communication Conference Technical Digest*, 2002, pp. 466–468.

[29] T. T. Larsen, A. Bjarklev, D. S. Hermann, and J. Broeng, "Optical devices based on liquid crystal photonic bandgap fibres," *Opt. Express*, vol. 11, pp. 2589–2596, Oct. 2003.

[30] S. G. Johnson and J. D. Joannopoulos, "Block-iterative frequency-domain methods for Maxwell's equations in a planewave basis," *Opt. Express*, vol. 8, pp. 173–190, Jan. 2001.

[31] T. Erdogan, "Fiber grating spectra," *J. Lightwave Technol.*, vol. 15, pp. 1277–1294, Aug. 1997.

[32] B. Y. Kim, J. N. Blake, H. E. Engan, and H. J. Shaw, "All-fiber acousto-optic frequency shifter," *Opt. Lett.*, vol. 11, pp. 389–391, June 1986.

[33] H. S. Kim, S. H. Yun, I. K. Kwang, and B. Y. Kim, "All-fiber acousto-optic tunable notch filter with electronically controllable spectral profile," *Opt. Lett.*, vol. 22, pp. 1476–1478, Oct. 1997.

[34] S. Ramachandran, "Dispersion-tailored few-mode fibers: A versatile platform for in-fiber photonic devices," *J. Lightwave Technol.*, vol. 23, pp. 3426–3443, Nov. 2005.

[35] B. J. Eggleton, P. S. Westbrook, C. A. White, C. Kerbage, R. S. Windeler, and G. L. Burdge, "Cladding-mode-resonances in air-silica microstructure optical fibers," *J. Lightwave Technol.*, vol. 18, pp. 1084–1100, Aug. 2000.

[36] A. Diez, T. A. Birks, W. H. Reeves, B. J. Mangan, and P. S. J. Russell, "Excitation of cladding modes in photonic crystal fibers by flexural acoustic waves," *Opt. Lett.*, vol. 25, pp. 1499–1501, Oct. 2000.

[37] D. Mogilevtsev, T. A. Birks, and P. S. J. Russell, "Group-velocity dispersion in photonic crystal fibers," *Opt. Lett.*, vol. 23, pp. 1662–1664, Nov. 1998.

[38] T. M. Monro, D. J. Richardson, N. G. R. Broderick, and P. J. Bennett, "Holey optical fibers: An efficient modal model," *J. Lightwave Technol.*, vol. 17, pp. 1093–1102, June 1999.

[39] N. A. Mortensen, M. D. Nielsen, J. R. Folkenberg, A. Petersson, and H. R. Simonsen, "Improved large-mode-area endlessly single-mode photonic crystal fibers," *Opt. Lett.*, vol. 28, pp. 393–395, Mar. 2003.

[40] M. Koshiba and K. Saitoh, "Applicability of classical optical fiber theories to holey fibers," *Opt. Lett.*, vol. 29, pp. 1739–1741, Aug. 2004.

[41] J. R. Folkenberg, N. A. Mortensen, K. P. Hansen, T. P. Hansen, H. R. Simonsen, and C. Jakobsen, "Experimental investigation of cutoff phenomena in nonlinear photonic crystal fibers," *Opt. Lett.*, vol. 28, pp. 1882–1884, Oct. 2003.

[42] B. T. Kuhlmey, R. C. McPhedran, and C. M. de Sterke, "Modal cutoff in microstructured optical fibers," *Optics Letters*, vol. 27, pp. 1684–1686, Oct. 2002.

[43] M. D. Nielsen, J. R. Folkenberg, and N. A. Mortensen, "Singlemode photonic crystal fibre with effective area of 600 μm^2 and low bending loss," *Electron. Lett.*, vol. 39, pp. 1802–1803, Dec. 2003.

[44] W. Jin, Z. Wang, and J. Ju, "Two-mode photonic crystal fibers," *Opt. Express*, vol. 13, pp. 2082–2088, Mar. 2005.

[45] T. Sørensen, J. Broeng, A. Bjarklev, E. Knudsen, S. E. B. Libori, H. R. Simonsen, and J. R. Jensen, "Macrobending loss properties of photonic crystal fibres with different air filling fractions," in *European Conference on Optical Communication*, Amsterdam, 2001, paper We.P.1.

[46] S. G. Leon-Saval, T. A. Birks, W. J. Wadsworth, P. S. J. Russell, and M. W. Mason, "Supercontinuum generation in submicron fibre waveguides," *Opt. Express*, vol. 12, pp. 2864–2869, June 2004.

[47] C. Kittel, *Introduction to solid state physics*. New York: Wiley, 1996.

[48] J. J. Sakurai, *Modern Quantum Mechanics*. Reading, Mass.: Addison-Wesley, 1994.

[49] K. Saitoh and M. Koshiba, "Leakage loss and group velocity dispersion in air-core photonic bandgap fibers," *Opt. Express*, vol. 11, pp. 3100–3109, Nov. 2003.

[50] A. Yariv and P. Yeh, *Optical Waves in Crystals*. New York: Wiley, 1984.

[51] H. E. Engan, B. Y. Kim, J. N. Blake, and H. J. Shaw, "Propagation and optical interaction of guided acoustic waves in two-mode optical fibers," *J. Lightwave Technol.*, vol. 6, pp. 428–436, Mar. 1988.

[52] K. F. Graff, *Wave motion in elastic solids*. Oxford: Clarendon, 1975.

[53] T. A. Birks, P. S. J. Russell, and D. O. Culverhouse, "The acousto-optic effect in single-mode fiber tapers and couplers," *J. Lightwave Technol.*, vol. 14, pp. 2519–2529, Nov. 1996.

[54] H. F. Taylor, "Bending effects in optical fibers," *J. Lightwave Technol.*, vol. LT-2, pp. 617–628, Oct. 1984.

[55] D. Östling and H. E. Engan, "Narrow-band acousto-optic tunable filtering in a two-mode fiber," *Opt. Lett.*, vol. 20, pp. 1247–1249, June 1995.

[56] H. S. Kim, S. H. Yun, H. K. Kim, N. Park, and B. Y. Kim, "Actively gain-flattened erbium-doped fiber amplifier over 35 nm by using all-fiber acoustooptic tunable filters," *IEEE Photon. Technol. Lett.*, vol. 10, pp. 790–792, June 1998.

[57] W. R. Trutna, Jr., D. W. Dolfi, and C. A. Flory, "Anomalous sidelobes and birefringence apodization in acousto-optic tunable filters," *Opt. Lett.*, vol. 18, pp. 28–30, Jan. 1993.

[58] D. A. Smith, A. d'Alessandro, J. E. Baran, and H. Herrmann, "Source of sidelobe asymmetry in integrated acousto-optic filters," *Appl. Phys. Lett.*, vol. 62, pp. 814–816, Feb. 1993.

[59] B. Langli, D. Östling, and K. Bløtekjær, "Axial variations in the acoustooptic phase-mismatch coefficient of two-mode fibers," *J. Lightwave Technol.*, vol. 16, pp. 2443–2450, Dec. 1998.

[60] D. G. Ouzounov, F. R. Ahmad, D. Müller, N. Venkataraman, M. T. Gallagher, M. G. Thomas, J. Silcox, K. W. Koch, and A. L. Gaeta, "Generation of megawatt optical solitons in hollow-core photonic bandgap fibers," *Science*, vol. 301, pp. 1702–1704, Sept. 2003.

[61] A. Mizrahi and L. Schächter, "Bragg reflection waveguides with a matching layer," *Opt. Express*, vol. 12, pp. 3156–3170, July 2004.

[62] P. Steinvurzel, E. D. Moore, E. C. Mägi, B. T. Kuhlmey, and B. J. Eggleton, "Long period grating resonances in photonic bandgap fiber," *Opt. Express*, vol. 14, pp. 3007–3014, Apr. 2006.

[63] P. Dainese, P. S. J. Russell, N. Joly, J. C. Knight, G. S. Wiederhecker, H. L. Fragnito, V. Laude, and A. Khelif, "Stimulated Brillouin scattering from multi-GHz-guided acoustic phonons in nanostructured photonic crystal fibres," *Nature Physics*, vol. 2, pp. 388–392, June 2006.

[64] T. T. Alkeskjold, "Optical devices based on liquid crystal photonic bandgap fibers," Ph.D. dissertation, Technical University of Denmark, Lyngby, May 2005.

[65] J. Lægsgaard, "Modeling of a biased liquid-crystal capillary waveguide," *J. Opt. Soc. Am. B*, vol. 23, pp. 1843–1851, Sept. 2006.

[66] D. C. Zografopoulos, E. E. Kriezis, and T. D. Tsiboukis, "Photonic crystal-liquid crystal fibers for single-polarization or high-birefringence guidance," *Opt. Express*, vol. 14, pp. 914–925, Jan. 2006.

[67] L. Scolari, T. T. Alkeskjold, J. Riishede, A. Bjarklev, D. S. Hermann, Anawati, M. D. Nielsen, and P. Bassi, "Continously tunable devices based on electrical control of dual-frequency liquid crystal filled photonic bandgap fibers," *Opt. Express*, vol. 13, pp. 7483–7496, Sept. 2005.

[68] T. T. Alkeskjold, J. Lægsgaard, A. Bjarklev, D. S. Hermann, Anawati, J. Broeng, J. Li, and S.-T. Wu, "All-optical modulation in dye-doped nematic liquid crystal photonic bandgap fibers," *Opt. Express*, vol. 12, pp. 5857–5871, Nov. 2004.

[69] V. V. Shevchenko, "Spectral expansions in eigenfunctions and associated functions of a non-self-adjoint Sturm-Liouville problem on the whole real line," *Differ. Equations.*, vol. 15, pp. 1431–1443, 1979.

[70] ——, "On the completeness of spectral expansion of the electromagnetic field in the set of dielectric circular rod waveguide eigen waves," *Radio Science*, vol. 17, pp. 229–231, 1982.

[71] J. M. Fini, "Suppression of higher-order modes in aircore microstructure fiber designs," in *Conference on Lasers and Electro-Optics*, Long Beach, CA, May 2006, paper CMM4.

Appendix A

Publication list

Journal papers

- B. Nistad, M. W. Haakestad, and J. Skaar, "Dispersion properties of planar Bragg waveguides," *Opt. Commun.*, vol. 265, pp. 153–160, Sep. 2006.[1]

- M. W. Haakestad and H. E. Engan, "Acoustooptic characterization of a birefringent two-mode photonic crystal fiber," *Opt. Express*, vol. 14, pp. 7319–7328, Aug. 2006.[1]

- M. W. Haakestad and H. E. Engan, "Acoustooptic properties of a weakly multimode solid core photonic crystal fiber," *J. Lightwave Technol.*, vol. 24, pp. 838–845, Feb. 2006.[1]

- M. W. Haakestad and J. Skaar, "Causality and Kramers–Kronig relations for waveguides," *Opt. Express*, vol. 13, pp. 9922–9934, Nov. 2005.[1]

- M. W. Haakestad, T. T. Alkeskjold, M. D. Nielsen, L. Scolari, J. Riishede, H. E. Engan, and A. Bjarklev, "Electrically tunable photonic bandgap guidance in a liquid-crystal-filled photonic crystal fiber," *IEEE Photon. Technol. Lett.*, vol. 17, pp. 819–821, Apr. 2005.[1]

- K. D. Knudsen, J. O. Fossum, G. Helgesen, and M. W. Haakestad, "Small-angle neutron scattering from a nano-layered synthetic silicate," *Physica B*, vol. 352, pp. 247–258, 2004.

[1]This paper is included in the thesis.

International conference presentations

- M. W. Haakestad and H. E. Engan, "Acoustooptic Characterization of a Birefringent Two-Mode Photonic Crystal Fiber," in *Optical Fiber Sensors Conference (OFS-18)*, Cancun, Mexico, Oct. 2006, paper ThA3.[2]

- M. W. Haakestad and J. Skaar, "Causality and Kramers–Kronig relations for waveguides," in *Conference on Lasers and Electro-Optics (CLEO)*, Long Beach, California, USA, May 2006, paper JWB57.[2]

- M. W. Haakestad and H. E. Engan, "Scaling properties of acousto-optic long period gratings in photonic crystal fibers," in *OSA Topical Meeting on Bragg Gratings, Poling & Photosensitivity (BGPP)*, Sydney, Australia, July 2005, Conference CD-ROM.[2]

- M. W. Haakestad, T. T. Larsen, M. D. Nielsen, H. E. Engan, and A. Bjarklev, "Electrically tunable fiber device based on a nematic liquid crystal filled photonic crystal fiber," in *30th European Conference on Optical Communication (ECOC)*, Stockholm, Sweden, Sept. 2004, postdeadline paper Th4.3.2.[2]

- M. W. Haakestad and H. E. Engan, "Acousto-optic properties of photonic crystal fibers," in *IEEE International Ultrasonics, Ferroelectrics, and Frequency Control Joint 50th Anniversary Conference*, Montréal, Canada, Aug. 2004, pp. 56–59.[2]

- K. D. Knudsen, J. O. Fossum, G. Helgesen, and M. W. Haakestad, "Pore characteristics and water absorption in a synthetic smectite clay," in *XII International Conference on Small-Angle Scattering*, Venice, Italy, Aug. 2002.

National conference presentations

- M. W. Haakestad and H. E. Engan, "Determination of axial variations in acoustooptic phase-mismatch coefficient of two-mode fibers from transmission spectrum," in *Northern Optics*, Bergen, Norway, June 2006, paper 060.[2]

[2]This item is a part of the Ph.D. work, but is not included in the thesis.

- D. D. Dang, A. Aksnes, M. W. Haakestad, J. K. Hagene, and O. Bjorøy, "Wavelength modulation spectroscopy with optical single mode fibers - a remote measurement of NH3 @ 1512nm," in *Northern Optics*, Bergen, Norway, June 2006, paper 160.

- K. D. Knudsen, J. O. Fossum, G. Helgesen, V. Bergaplass, and M. W. Haakestad, "Pore characteristics and pressure effects in a nano-layered silicate," in *Annual Meeting of The Division for Condensed Matter Physics with Atomic Physics*, Wadahl, Norway, Sept. 2004.

- M. W. Haakestad and H. E. Engan, "Acousto-optic interaction in photonic crystal fibers," in *The Norwegian Electro-optics Meeting*, Tønsberg, Norway, May 2004.[2]

- B. Nistad, M. W. Haakestad, and J. Skaar, "Dispersion properties of symmetric Bragg slab waveguides," in *The Norwegian Electro-optics Meeting*, Tønsberg, Norway, May 2004.[2]

- M. W. Haakestad and H. E. Engan, "Acousto-optic interaction in photonic crystal fibers," in *27th Scandinavian Symposium on Physical Acoustics*, Ustaoset, Norway, Jan. 2004.[2]

- G. Arisholm, K. Stenersen, G. Rustad, E. Lippert, and M. W. Haakestad, "Mid-infrared optical parametric oscillators based on periodically-poled lithium niobate," in *The Norwegian Electro-optics Meeting*, Flåm, Norway, May 2002.

- M. W. Haakestad, K. D. Knudsen, G. Helgesen, T. N. Aalerud, and J. O. Fossum, "Small-angle neutron-scattering studies of a synthetic clay: Sodium Fluorohectorite," in *The Norwegian Physics Conference*, Trondheim, Norway, June 2001.

Appendix B

Included papers